Adaptive Modulation Schemes for Visible Light Communications

Liang Wu, *Member, IEEE*, Zaichen Zhang, *Member, IEEE*, Jian Dang, and Huaping Liu, *Senior Member, IEEE*

***Abstract*—A major limitation of existing visible light communication (VLC) systems is the limited modulation bandwidth of light-emitting diodes used in such systems. Using adaptive modulation to improve the spectral efficiency for radio communications has been well studied. For VLC with various physical layer schemes, however, how adaptive modulation works is not well understood yet. The goal of this paper is to provide an in-depth analysis of the achievable spectral efficiency of adaptive modulation for three different schemes for high speed VLC: dc-biased optical orthogonal frequency division multiplexing (DCO-OFDM), asymmetrically clipped optical OFDM (ACO-OFDM), and single-carrier frequency-domain equalization (SC-FDE). We will show that in the low signal-to-noise ratio region, the ACO-OFDM-based adaptive modulation scheme outperforms the other two schemes. SC-FDE-based adaptive modulation achieves a better performance than the DCO-OFDM-based scheme, and it is much simpler than the other two schemes.**

***Index Terms*—Adaptive modulation, orthogonal frequency division multiplexing (OFDM), single-carrier frequency-domain equalization (SC-FDE), visible light communication (VLC).**

I. Introduction

VISIBLE light communication (VLC) has gained significant attention in both academia and industry recently [1], [2]. Intensity modulation with direct detection (IM/DD) is typically used in VLC systems because of its simplicity. In IM/DD VLC systems, signals are transmitted through a light-emitting diode (LED) in the form of optical power, which means that the modulated signal is nonnegative. In the receiver, a photo detector (PD) is employed to convert the optical power signal into electrical signals. A limitation of VLC systems is their limited modulation bandwidth determined by the LED, which is typically in the range of tens of MHz (3-dB bandwidth) only [3]. The equivalent channel for VLC systems is a low-pass channel, which will cause inter-symbol interference (ISI) for high-speed transmission. However, ISI mitigation schemes developed for radio frequency (RF) communications cannot be directly applied to IM/DD VLC systems [4]. Modified orthogonal frequency division multiplexing (OFDM) schemes have been proposed for VLC; for example, DC-biased optical OFDM (DCO-OFDM) and asymmetrically clipped optical OFDM (ACO-OFDM) are studied in [5] and [6], respectively. In DCO-OFDM systems, a DC bias is added to the normal OFDM symbol to reduce the amount of signal distortion and noise induced by negative clipping. In ACO-OFDM, only the odd indexed subcarriers are modulated; the negative signals are clipped to zero during transmission.

It is well known that adaptive modulation could improve the spectral efficiency. Many adaptive transmission techniques have been presented in the literature. The combination of adaptive modulation with OFDM, which is also known as bit and power loading, was proposed in 1989 by Kalet [7] and further developed by Chow [8] and Czylwik [9]. There are three common types of adaptive modulations [10]: variable rate variable power systems; variable rate constant power systems; and constant rate variable power systems. DCO-OFDM based adaptive modulation scheme is also applied for infrared communications [11]. For VLC, however, not much work has studied the use of adaptive modulation.

In VLC systems, a constant transmitted optical power is preferred for luminance considerations. The goal of this paper is to provide an in-depth analysis of adaptive modulation for three VLC systems assuming variable rate constant optical power (VRCOP) and perfect channel state information (CSI) at both the transmitter and receiver. Here VRCOP targets to maximize the spectral efficiency under the constraints of optical power and a target bit error rate (BER). Specifically, the maximum achievable spectral efficiency will be derived for DCO-OFDM and ACO-OFDM adaptive modulation systems given a target BER. Besides, a single-carrier frequency-domain equalization (SC-FDE) based adaptive modulation scheme for VLC is proposed and its achieved spectral efficiency is derived. Compared with the other two schemes, this scheme has a a lower computational complexity and a significantly lower feedback overhead. Also, its achieved spectral efficiency is higher in the high signal-to-noise ratio (SNR) region.

II. Signal Model

The VLC channel can be described as a flat fading channel or a diffuse channel, depending on the link conditions. The physical channel model includes both the line-of-sight (LOS) and the diffuse components. The channel impulse response is modeled as [12]

$$h(t) = \eta_{\mathrm{LOS}}\delta(t) + h_{\mathrm{diffuse}}(t - \Delta\tau) \tag{1}$$

Manuscript received July 11, 2014; revised November 17, 2014; accepted November 18, 2014. Date of publication November 23, 2014; date of current version December 16, 2014. This work was supported by 863 Project 2013AA013601, NSFC Project 61223001, Jiangsu NSF Project BK20140646, the Research Fund of NCRL (2014A03, 2014B03, and 2014B04), the Research Fund of ZTE Corporation, the Fundamental Research Funds of the Central Universities (2242014K40033), and the PRPFN of Jiangsu FNII (BY2013095-1-18).

L. Wu, Z. Zhang and J. Dang are with the National Mobile Communications Research Laboratory, Southeast University, Nanjing 210096, China (e-mail: wuliang@seu.edu.cn; zczhang@seu.edu.cn; newwanda@seu.edu.cn).

H. Liu is with the School of Electrical Engineering and Computer Science, Oregon State University, Corvallis OR 97331 USA (e-mail: hliu@eecs.oregonstate.edu).

Color versions of one or more of the figures in this paper are available online at http://ieeexplore.ieee.org.

Digital Object Identifier 10.1109/JLT.2014.2374171

where η_{LOS} is the LOS component, $\delta(t)$ is Dirac delta function, $h_{\mathrm{diffuse}}(t)$ is the diffuse component, and $\Delta\tau$ is the delay between the LOS signal and the diffuse signal. The LOS component is expressed as

$$\eta_{\mathrm{LOS}} = \begin{cases} \dfrac{(m+1)A_r\cos(\varphi)}{2\pi D^2}\cos^m(\theta)T(\varphi)G(\varphi) & \varphi < \Psi \\ 0 & \varphi > \Psi \end{cases} \tag{2}$$

where A_r is the detection area of the PD, and D and φ are, respectively, the distance and angle of incidence form the LED to the PD, $T(\varphi)$ and $G(\varphi)$ are, respectively, the optical filter gain and the concentrator gain of the receiver, Ψ is the field of view (FOV) of the receiver, θ is the angle of irradiance from the LED to the PD, and m is the order of Lambertian emission, which is related to the semiangle at half-power of the transmit LED, $\Phi_{1/2}$, as $m = -\ln 2/\ln(\cos\Phi_{1/2})$.

In the frequency domain, the diffuse component is [12]

$$H_{\mathrm{diffuse}}(f) = \frac{\eta_{\mathrm{diffuse}}}{1 + j\frac{f}{f_0}} \tag{3}$$

where f_0 is the 3-dB cut off frequency, and η_{diffuse} is expressed as

$$\eta_{\mathrm{diffuse}} = \frac{A_r}{A_{\mathrm{room}}}\frac{\rho_1}{1-\rho} \tag{4}$$

where A_{room} is the area of the room surface, ρ_1 is the reflectivity of the region initially illuminated by the transmitter, ρ is the average reflectivity of the walls. In this paper $\rho_1 = \rho$ as in [12] will be assumed.

One major limitation of VLC is the limited modulation bandwidth of the LED, which will cause ISI for high speed transmission. The normalized impulse response of the LED is [3]

$$g(t) = e^{-2\pi f_b t} \tag{5}$$

where f_b is the 3-dB modulation bandwidth of the LED. We define the equivalent channel as

$$h_{eq}(t) = rh(t) \otimes g(t) \tag{6}$$

where r is the responsivity of PD. At the receiver, the received signal in the discrete form can be expressed as

$$y(n) = s(n) \otimes h_{eq}(n) + z(n) \tag{7}$$

where $s(n)$ is the transmitted signal, $h_{eq}(n)$ is the discrete form of $h_{eq}(t)$, and $z(n)$ is a noise component. The noise component $z(n)$ consists of thermal noise, relative-intensity noise and shot noise, and can be modeled as a white Gaussian noise with zero mean and variance σ_z^2[13].

III. Adaptive Modulation for VLC

If adaptive modulation is implemented with the various VLC schemes, how each of them works? In this section we analyze in detail three VLC adaptive modulation schemes in terms of the channel capacity, the achieved rate, and the BER.

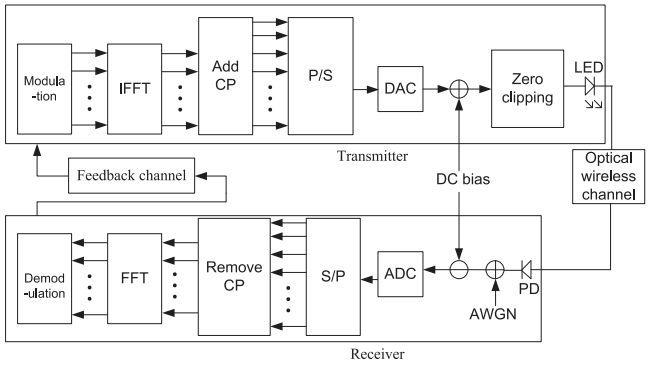

Fig. 1. Block diagram of the VLC system that employs DCO-OFDM with adaptive modulation.

A. DCO-OFDM Based Adaptive Modulation Scheme

DCO-OFDM is a form of OFDM with a DC bias aided. In such systems, the frequency domain signal is transformed into the time domain by using the inverse discrete Fourier transform, which can be implemented by using an inverse fast Fourier transform (IFFT). The length of the IFFT is assumed to be N. The modulated signal in the frequency domain must be conjugate symmetric [5] to ensure that the time domain signal is real. Finally, a DC bias is added to guarantee that the transmitted signals are nonnegative.

The block diagram of a DCO-OFDM VLC system is shown in Fig. 1. The modulated signals in the frequency domain satisfy the following conditions:

$$\begin{cases} X(0) = X(\frac{N}{2}) = 0 \\ X(K) = X^*(N-K), \quad K = 1, 2, \ldots, N-1 \end{cases} \tag{8}$$

where N is the size of IFFT. After IFFT, the time domain signal can be expressed as

$$\begin{aligned} x(n) &= \frac{1}{N}\sum_{K=0}^{N-1} X(K)e^{j\frac{2\pi K n}{N}} \\ &= \frac{1}{N}\sum_{K=1}^{N/2-1} X(K)e^{j\frac{2\pi K n}{N}} + \frac{1}{N}\sum_{K=N/2+1}^{N-1} X(K)e^{j\frac{2\pi K n}{N}} \\ &= \frac{1}{N}\sum_{K=1}^{N/2-1}\left(X(K)e^{j\frac{2\pi K n}{N}} + X^*(K)e^{-j\frac{2\pi K n}{N}}\right) \\ &= \frac{2}{N}\sum_{K=1}^{N/2-1}\left(a(K)\cos\left(\frac{2\pi K n}{N}\right)\right. \\ &\quad \left. -b(K)\sin\left(\frac{2\pi K n}{N}\right)\right). \end{aligned} \tag{9}$$

It is assumed that $X(K) = a(K) + jb(k)$ is a zero mean complex random variable with variance σ_K^2, $X(K), K = 1, \cdots, N/2-1$, are independent, and $a(k)$ and $b(K)$ are independent real random variables with a mean zero

and variance $\sigma_K^2/2$. According to the law of large numbers, $x(n)$ is a Gaussian random variable with zero mean [15], that is $E[x(n)] = 0$, where $E[\cdot]$ stands for expectation.

In the DCO-OFDM system, the variance of the time domain signal $x(n)$ can be derived from Eq. (9) as

$$\begin{aligned}\sigma_x^2 =& \ E[(x(n))^* x(n)] \\ =& \ \frac{4}{N^2}\sum_{K=1}^{N/2-1}\left(\frac{\sigma_K^2}{2}\cos^2\left(\frac{2\pi Kn}{N}\right)\right. \\ &\left. +\frac{\sigma_K^2}{2}\sin^2\left(\frac{2\pi Kn}{N}\right)\right) = \frac{2}{N^2}\sum_{K=1}^{N/2-1}\sigma_K^2 \end{aligned} \quad (10)$$

where $(\cdot)^*$ stands for conjugation.

The DC bias can be set to be $\lambda\sigma_x$, where λ is a positive real number. The transmitted signal takes the form:

$$\begin{aligned} s(n) =& \ (x(n) + \lambda\sigma_x)^+. \\ =& \ x(n) + \lambda\sigma_x - e_c(n) \end{aligned} \quad (11)$$

where, $(y)^+ = \max\{0, y\}$ and $e_c(n)$ is a clipping noise.

For a zero mean Gaussian random variable v with variance σ_ν^2, the probability that v lies in $[-2\sigma_\nu, 2\sigma_\nu]$ is about 95.6% [15]. Therefore,

$$\Pr(v + 2\sigma_\nu > 0) \approx 97.8\% \quad (12)$$

which is very close to 1. After zero clipping, the probability and probability density of clipping noise $e_c(n)$ take the form

$$\Pr(e_c(n) = u) = \ 1 - Q(\lambda) \qquad u = 0 \quad (13a)$$

$$f_{e_c(n)}(u) = \ \frac{1}{\sqrt{2\pi\sigma_x^2}} e^{-\frac{(u-\lambda\sigma_x)^2}{2\sigma_x^2}} \quad u < 0 \quad (13b)$$

where $Q(x) = \frac{1}{\sqrt{2\pi}}\int_x^\infty \exp(-\frac{u^2}{2})du$ is the Q-function. The average transmitted optical power is expressed as

$$E[s(n)] = \sigma_x \underbrace{\left(\lambda + \frac{1}{\sqrt{2\pi}}e^{-\lambda^2/2} - \lambda Q(\lambda)\right)}_{\triangleq \kappa} \quad (14)$$

where $\triangleq$ stands for definition.

The clipping noise, which will affect performance[16], is not well understood yet, but it is generally accepted that it is approximately uncorrelated with $x(n)$ [17], [18]. Note that for a large bias, the effect of clipping noise can be ignored in the moderate SNR region. In this paper, λ chosen as $\lambda \geq 1.5$, which represents the scenario of a large bias according to Eq. (12). DCO-OFDM is a form of OFDM, with which the modulated signals in the frequency domain satisfy the conditions given by Eq. (8). Therefore, The channel capacity (bit per second/Hz, bps/Hz) of the DCO-OFDM system can be expressed as [19], [20]

$$R_{\max}^{\mathrm{DCO}} = \frac{N}{N+N_{cp}}\frac{1}{N}\sum_{K=1}^{N/2-1}\log_2\left(1 + \frac{|H_{eq}(K)|^2\sigma_K^2}{\sigma_Z^2}\right) \quad (15)$$

subject to (optical power constraint)

$$0 \leq E[s(n)] \leq p_x \quad (16)$$

where, N_{cp} is the length of cyclic prefix (CP), $H_{eq}(K) = \sum_{K=0}^{N-1} h_{eq}(n)e^{-j\frac{2\pi Kn}{N}}$, σ_Z^2 is the variance of $Z(K) = \sum_{K=0}^{N-1} z(n)e^{-j\frac{2\pi Kn}{N}}$, $\sigma_Z^2 = N\sigma_z^2$, and p_x is a constant.

From Eqs. (10), (14), and (16), the electrical power constraint is

$$\frac{2}{N^2}\sum_{K=1}^{N/2-1}\sigma_K^2 \leq \frac{p_x^2}{\kappa^2}. \quad (17)$$

For a specific optical power constraint, which can be transformed into electrical power constraint, the channel capacity can be achieved by using water-filling [19]. The constraint can be rewritten in the following form:

$$\begin{aligned}\sum_{K=1}^{N/2-1}\frac{\sigma_K^2}{\sigma_Z^2} =& \ \frac{1}{N\sigma_z^2}\sum_{K=1}^{N/2-1}\sigma_K^2 \\ \leq& \ \frac{Np_x^2}{2\kappa^2\sigma_z^2}\end{aligned} \quad (18)$$

where p_x/σ_z is defined as optical SNR.

We assume an M-ary quadrature amplitude modulation (QAM) ($M = 2^k, k = 1, 2, \cdots, \Xi_{\mathrm{DCO}}$) for the DCO-OFDM VLC system. A unified expression of the approximate BER of M-QAM signals over an additive Gaussian noise channel is written as [21]

$$\Pr(M, \gamma_{\mathrm{rec}}) \approx 0.2\exp(-\psi(M)\gamma_{\mathrm{rec}}) \quad (19)$$

where γ_{rec} is the received electrical SNR and $\psi(M)$ is a constellation-specific quantity defined as

$$\psi(M) = \begin{cases} 1.5/(M-1) & \text{for square } M\text{-QAM} \\ 6/(5M-4) & \text{for rectangular } M\text{-QAM.} \end{cases} \quad (20)$$

Considering a certain BER target and Eq. (19), we define the SNR threshold as

$$\mathrm{th}_k = -\frac{\ln(5\mathrm{BER_t})}{\psi(2^k)}, \quad k = 1, 2, \ldots, \Xi_{\mathrm{DCO}} \quad (21)$$

where $\mathrm{th}_1 < \mathrm{th}_2 < \cdots < \mathrm{th}_{\Xi_{\mathrm{DCO}}}$.

The corresponding SNR thresholds of the modulated subcarriers can be expressed as

$$\begin{aligned}\mathrm{ThSNR}_{K,j} =& \ \frac{\mathrm{th}_j}{|H_{eq}(K)|^2}, \\ & K = \ 1, \ldots, N/2-1 \,; j = 1, \ldots, \Xi_{\mathrm{DCO}}.\end{aligned} \quad (22)$$

The achieved spectral efficiency of the K-th modulated subcarrier is

$$R_K = \sum_{i=1}^{\Xi_{\mathrm{DCO}}} U\left(\frac{\sigma_X^2}{\sigma_Z^2} - \mathrm{ThSNR}_{K,i}\right). \quad (23)$$

According to the optimal power allocation policy, the aim of adaptive modulation is to maximize the achieved spectral

efficiency under the BER target and optical power constraints. The optimization problem can be expressed as (OP1):

$$\max_{\sigma_K^2/\sigma_Z^2} \left\{ \sum_{K=1}^{N/2-1} \sum_{i=1}^{\Xi_{\mathrm{DCO}}} U\left(\frac{\sigma_K^2}{\sigma_Z^2} - \mathrm{ThSNR}_{K,i} \right) \right\} \tag{24}$$

subject to

$$\sum_{K=1}^{N/2-1} \frac{\sigma_K^2}{\sigma_Z^2} \leq \frac{N p_x^2}{2\kappa^2 \sigma_z^2}. \tag{25}$$

To maximize power efficiency, the power allocated to each subcarrier only needs to satisfy

$$\frac{\sigma_K^2}{\sigma_Z^2} \in \left\{ \mathrm{ThSNR}_{K,i}, \quad i = 1, 2, \ldots, \Xi_{\mathrm{DCO}} \right\}. \tag{26}$$

Let us define the incremental SNR as

$$\Delta_{K,i}^{\mathrm{SNR}} = \begin{cases} \mathrm{ThSNR}_{\mathrm{K},1} & \mathrm{i} = 1 \\ \mathrm{ThSNR}_{K,i} - \mathrm{ThSNR}_{K,i-1} & i = 2, \ldots, \Xi_{\mathrm{DCO}} \end{cases} \tag{27}$$

where $\Delta_{K,i}^{\mathrm{SNR}} \leq \Delta_{K,i+1}^{\mathrm{SNR}}$ for each subcarrier. If the modulation of the K-th subcarrier is 2^{R_K} -QAM, then the electrical SNR is $\mathrm{SNRe}_K = \sum_{i=1}^{R_K} \Delta_{K,i}^{\mathrm{SNR}}$.

Consequently, OP1 is equivalent to the following optimization problem (OP2):

$$\max_{R_k} \left\{ R_{\mathrm{total}}^{\mathrm{DCO}} = \sum_{K=1}^{N/2-1} R_K \right\} \tag{28}$$

subject to

$$\sum_{K=1}^{N/2-1} \sum_{i=1}^{R_K} \Delta_{K,i}^{\mathrm{SNR}} \leq \frac{N p_x^2}{2\kappa^2 \sigma_z^2}. \tag{29}$$

According to [22], OP2 can be solved through the following two steps:

	(Algorithm 1):
1	Sort the $\left(\frac{N}{2}-1\right) \cdot \Xi_{\mathrm{DCO}}$ values of $\Delta_{K,i}^{\mathrm{SNR}}$ for $(K = 1, 2 \ldots, N/2 - 1; i = 1, 2 \ldots, \Xi_{\mathrm{DCO}})$ in ascending order expressed as $\Upsilon_1 \leq \Upsilon_2 \leq \cdots \leq \Upsilon_{(N/2-1)\Xi_{\mathrm{DCO}}}$.
2	Find the maximum value of $R_{\mathrm{total}}^{\mathrm{DCO}}$, subject to $\sum_{i=1}^{R_{\mathrm{total}}^{\mathrm{DCO}}} \Upsilon_i \leq \frac{N p_x^2}{2\kappa^2 \sigma_z^2}$.

Let $2^{R_{K,\mathrm{opt}}}$-QAM denote the optimal modulation scheme for the K-th subcarrier. The electrical SNR of the K-th subcarrier is determined to be

$$\mathrm{SNRe}_K = \begin{cases} \sum_{i=1}^{R_{K,\mathrm{opt}}} \Delta_{K,i}^{\mathrm{SNR}} & R_{K,\mathrm{opt}} \geq 1 \\ 0 & R_{K,\mathrm{opt}} = 0. \end{cases} \tag{30}$$

The achieved spectral efficiency (bps/Hz) of DCO-OFDM based adaptive modulation scheme is

$$R_{\mathrm{achieve}}^{\mathrm{DCO}} = \frac{N}{N + N_{cp}} \frac{1}{N} \sum_{K=1}^{N/2-1} R_{K,\mathrm{opt}}. \tag{31}$$

To realize the DCO-OFDM based adaptive modulation algorithm, either CSI or the modulation orders and power allocation strategy need be sent back to the transmitter. When CSI is sent to the transmitter, the receiver will need to determine the modulation order of each subcarrier first and then performs proper demodulation scheme for each subcarrier. Therefore, the receiver complexity will be high. When the modulation order and power allocation strategy for each subcarrier is sent back to the transmitter, the required amount of feedback information is generally high.

B. ACO-OFDM Based Adaptive Modulation Scheme

ACO-OFDM signals can be transmitted without resorting to a DC-bias. In such a system, only the odd indexed subcarriers are modulated and the even indexed subcarriers are set to zeros. After IFFT, the time domain signal satisfies [6]

$$x\left(n + \frac{N}{2}\right) = -x(n) \quad n = 0, \ldots, \frac{N}{2} - 1. \tag{32}$$

The transmitted signal in an ACO-OFDM system can be expressed as

$$s(n) = \begin{cases} x(n) & x(n) > 0 \\ 0 & x(n) \leq 0. \end{cases} \tag{33}$$

The probability and probability density functions of $s(n)$ are written as

$$\Pr(s(n) = u) = 0.5 \qquad u = 0 \tag{34a}$$

$$f_{s(n)}(u) = \frac{1}{\sqrt{2\pi\sigma_x^2}} e^{-\frac{u^2}{2\sigma_x^2}} \quad u > 0. \tag{34b}$$

The expectation of $s(n)$ is

$$\begin{aligned} E[s(n)] &= 0.5 \times 0 + \int_0^{+\infty} u \frac{1}{\sqrt{2\pi\sigma_x^2}} e^{-\frac{u^2}{2\sigma_x^2}} du \\ &= \frac{\sigma_x}{\sqrt{2\pi}}. \end{aligned} \tag{35}$$

Same as the DCO-OFDM system, $X(K)$ assumed to be a zero mean random variable with variance σ_K^2, and $x(n)$ is a zero mean Gaussian random variable. The variance of $x(n)$ is written as

$$\sigma_x^2 = \frac{2}{N^2} \sum_{K=1}^{N/4} \sigma_{2K-1}^2 \tag{36}$$

where σ_{2K-1}^2 is the variance of $X(2K-1)$.

In the detection phase of ACO-OFDM systems, the received signal in the frequency domain is scaled by a factor of 2 [6], which enlarges the noise variance by a factor of 4. For an average transmitted optical power of p_x, the channel capacity of ACO-OFDM VLC systems can be expressed as

$$\begin{aligned} R_{\max}^{\mathrm{ACO}} &= \frac{N}{N + N_{cp}} \frac{1}{N} \\ &\quad \cdot \sum_{K=1}^{N/4} \log_2 \left(1 + \frac{|H_{eq}(2K-1)|^2 \sigma_{2K-1}^2}{4\sigma_Z^2} \right) \end{aligned} \tag{37}$$

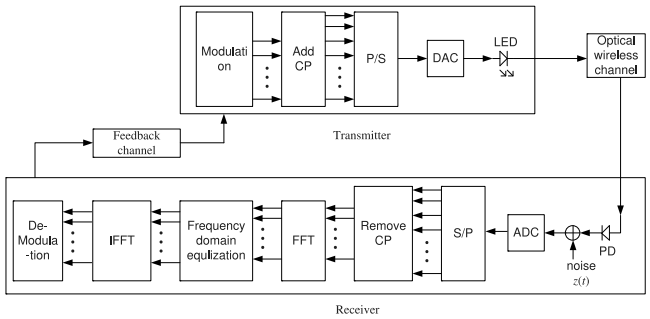

Fig. 2. Block diagram of the VLC system that employs SC-FDE with adaptive modulation.

subject to (optical power constraint)

$$0 \le E[s(n)] \le p_x. \tag{38}$$

From Eqs. (35), (36), and (38), the constraint in the electrical domain is

$$\frac{2}{N^2}\sum_{K=1}^{N/4}\sigma_{2K-1}^2 \le 2\pi p_x^2. \tag{39}$$

The channel capacity can be achieved through water-filling [19]. The constraint in the form of electrical SNR is

$$\sum_{K=1}^{N/4}\frac{\sigma_{2K-1}^2}{4\sigma_Z^2} = \frac{1}{4N\sigma_z^2}\sum_{K=1}^{N/4}\sigma_{2K-1}^2 \le \frac{N\pi}{4}\frac{p_x^2}{\sigma_z^2}. \tag{40}$$

The optimal adaptive modulation scheme in the ACO-OFDM system can be expressed as the following optimization problem (OP3):

$$\max\left\{R_{\text{total}}^{\text{ACO}} \triangleq \sum\nolimits_{K=1}^{N/4} R_{2K-1}\right\} \tag{41}$$

subject to

$$\sum_{K=1}^{N/4}\sum_{j=1}^{R_{2i-1}}\Delta_{2K-1,j}^{\text{SNR}} \le \frac{N\pi}{4}\frac{p_x^2}{\sigma_z^2}. \tag{42}$$

The problem can be solved by using Algorithm 1.

The achieved spectral efficiency of the ACO-OFDM based adaptive modulation scheme is

$$R_{\text{achieve}}^{\text{ACO}} = \frac{N}{N+N_{cp}}\frac{1}{N}\sum_{K=1}^{N/4-1}R_{2K-1,\text{opt}}. \tag{43}$$

Similar to DCO-OFDM based adaptive modulation, to realize the ACO-OFDM based adaptive modulation algorithm, either CSI or the modulation order and power allocation strategy for each subcarrier must be sent to the transmitter. The complexities of the ACO-OFDM based adaptive modulation scheme and the DCO-OFDM based adaptive modulation scheme are similar.

C. SC-FDE Based Adaptive Modulation Scheme

SC-FDE is another effective method to combat ISI [23]. The block diagram of SC-FDE is shown in Fig. 2. After frequency domain equalization, the signal on the K-th subcarrier is

$$\tilde{Y}(K) = X(K) + \frac{Z(K)}{H(K)}. \tag{44}$$

The corresponding time domain signal is

$$\tilde{y}(n) = x(n) + \tilde{z}(n) \tag{45}$$

where the noise component $\tilde{z}(n)$ is

$$\tilde{z}(n) = \frac{1}{N}\sum_{K=0}^{N-1}\frac{Z(K)}{H(K)}e^{j\frac{2\pi}{N}Kn} \tag{46}$$

with the variance

$$\sigma_{\tilde{z}}^2 = \frac{\sigma_z^2}{N}\sum_{K=0}^{N-1}\frac{1}{|H(K)|^2}. \tag{47}$$

After frequency domain equalization, the channel can be considered flat. For an average transmitted optical power of p_x, the lower bound on the channel capacity of SC-FDE systems can be expressed as [24]

$$R_{\max}^{\text{SC-FDE}} \ge \frac{N}{N+N_{cp}}\frac{1}{2}\log_2\left(1+\frac{e}{\frac{2\pi}{N}\sqrt{\sum_{K=0}^{N-1}\frac{1}{|H(K)|^2}}}\cdot\frac{p_x^2}{\sigma_z^2}\right). \tag{48}$$

When M-ary pulse amplitude modulation (M-PAM) with Gray code mapping is employed, the BER over an AWGN channel is approximated as [14]

$$\text{BER}_{\text{PAM}}(M,\text{SNRo}) \approx \frac{2(M-1)}{M\log_2 M}Q\left(\frac{\text{SNRo}}{(M-1)}\right) \tag{49}$$

where $\text{SNRo} = p_x/\sigma_{\tilde{z}}$ is the optical SNR, which is defined as the ratio of optical signal power and noise standard deviation. When the BER target is BER_t, the modulation thresholds are

$$\begin{aligned}\text{Th}_i &= (\text{SNRo})_M \\ &= (M-1)Q^{-1}\left(\text{BER}_\text{t}\frac{M\log_2 M}{2(M-1)}\right) \\ &\qquad M = 2^i,\ \ i = 1,\ldots,\Xi_{\text{SC}}\end{aligned} \tag{50}$$

where $Q^{-1}(\cdot)$ is the inverse Q-function, and

$$\text{Th}_1 \le \text{Th}_2 \le \cdots \le \text{Th}_{\Xi_{\text{SC}}}. \tag{51}$$

The modulation order can be chosen according to SNRo as

$$M = \begin{cases} 0, & \text{SNRo} < \text{Th}_1 \\ 2^i, & \text{Th}_i \le \text{SNRo} < \text{Th}_{i+1}, i = 1,2,\ldots,\Xi_{\text{SC}}-1 \\ 2^{\Xi_{\text{SC}}}, & \text{Th}_{\Xi_{\text{SC}}} \le \text{SNRo}. \end{cases} \tag{52}$$

For example, if $\text{Th}_3 \le \text{SNRo} < \text{Th}_4$, then the modulation scheme is 8-PAM. The achieved spectral efficiency can be expressed as

$$R_{\text{achieve}}^{\text{SC-FDE}} = \frac{N}{N+N_{cp}}\sum_{i=1}^{\Xi_{\text{SC}}}U(\text{SNRo}-\text{Th}_i). \tag{53}$$

The above analysis shows that only the modulation order, which will be fixed during transmission, needs to be sent to

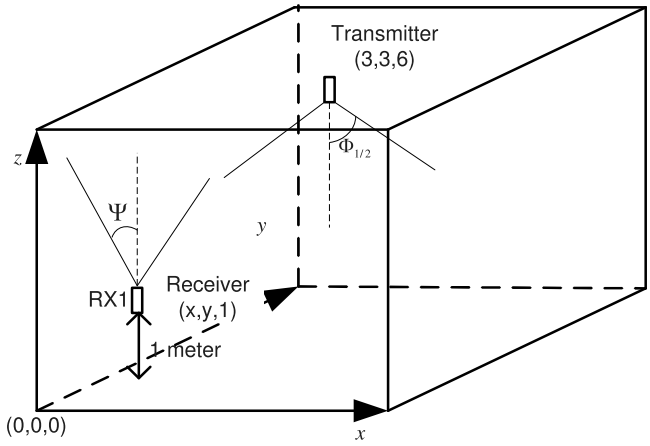

Fig. 3. Visible light communication model in a room.

TABLE I
SYSTEM PARAMETERS

Semiangle at half power $\Phi_{1/2}$	40 deg
FOV at receiver Ψ	60 deg
Detector area A_r	1.0 cm^2
Optical filter gain $T(\varphi)$	1.0
Concentrator gain $G(\varphi)$	1.0
Photodiode responsivity r	1
Walls average reflectivity ρ	0.43

the transmitter. For example when Ξ_{SC}-PAM is employed, only $\log_2(\Xi_{\mathrm{SC}})$ bits are needed to be sent to the transmitter. Also, the modulation orders of different PAM symbols in one frame are the same. Therefore, the complexity of SC-FDE based adaptive modulation scheme is lower than that of OFDM based adaptive modulation schemes.

IV. SIMULATION RESULTS

In the simulation, the 3-dB bandwidth of the equivalent channel is set to be 10 MHz, and the employed modulated bandwidth is 100 MHz, which means that the subcarrier spacing is $100/N$ MHz with $N = 512$. The PAM symbol rate in SC-FDE systems is 100 Msymbol/s. Therefore, ISI exists in this system. The length of CP is $N_{cp} = 8$ for the three schemes; that is the length of CP in the time domain is 80ns, which is greater than the delay spread of the equivalent channel. SNR is defined according to the transmitted optical power as $\mathrm{SNR} = E[s(n)]/\sigma_z$. The configuration of the system is shown in Fig. 3. The room size is $6\,\mathrm{m} \times 6\,\mathrm{m} \times 6\,\mathrm{m}$. The coordinate of the transmitter is $(3, 3, 6)$, which is located at the center of the ceiling, and the receiver is located at 1 meter above the ground. Other system parameters are given in Table I. The DC gain of the channel is calculated based on the given parameters. In the simulation environment, an LOS link is established.

We will first evaluate the effect of the DC bias in the DCO-OFDM based adaptive modulation system. The receiver is located at $(1.5, 2.5, 1)$. Fig. 4 shows the achieved spectral efficiency of this scheme with different DC biases. It is observed from Fig. 4 that a lower DC bias achieves a higher spectral

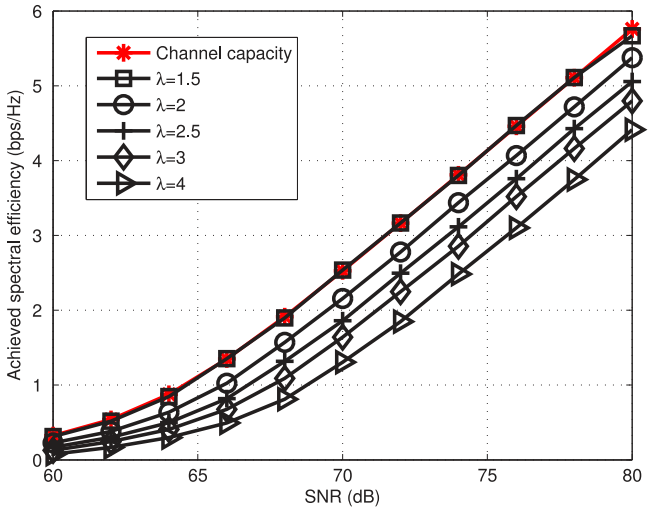

Fig. 4. Achieved spectral efficiency of DCO-OFDM adaptive modulation system with different DC biases (receiver at $(1.5, 2.5, 1)$).

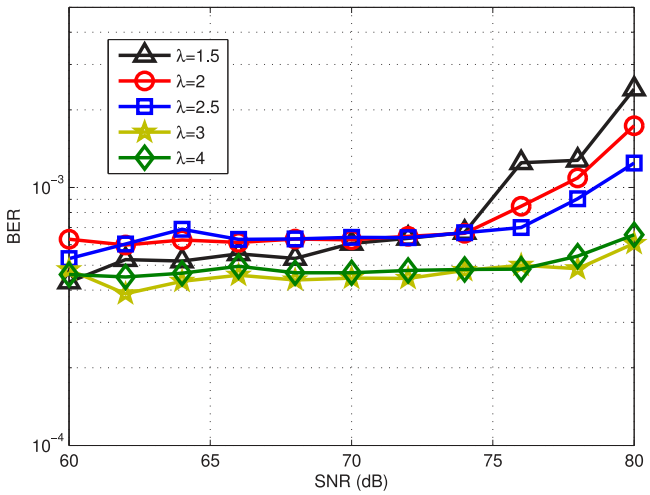

Fig. 5. Simulated BER performance of the DCO-OFDM adaptive modulation system with different DC biases (receiver at $(1.5, 2.5, 1)$).

efficiency, because the DC bias is assumed to be large enough so that the clipping noise can be ignored. The BER performance is affected by clipping noise, when it is considered in the simulation, as shown in Fig. 5. The BER target might not be met with a low DC bias. Fig. 5 shows the simulated BER performance with different DC biases. It shows that the optimal DC bias value varies for different SNR values. When SNR is lower than 75 dB, the optimal DC bias is about $1.5\sigma_x$, which achieves the highest spectral efficiency and still satisfy the BER target; when SNR is in the region of $75 - 77$ dB, the optimal DC bias is about $2\sigma_x$. When λ is greater than 2.5, the BER can be satisfied (below 10^{-3}) in the whole simulated SNR region.

Fig. 6 shows the bits loaded on each modulated subcarrier in the DCO-OFDM adaptive modulation system. Here SNR $=$ 75 dB and the receiver is located at $(1.5, 2.5, 1)$. It shows that a higher modulation order is employed in the lower frequency subcarriers, because of the low-pass property of the LED. Fig. 7

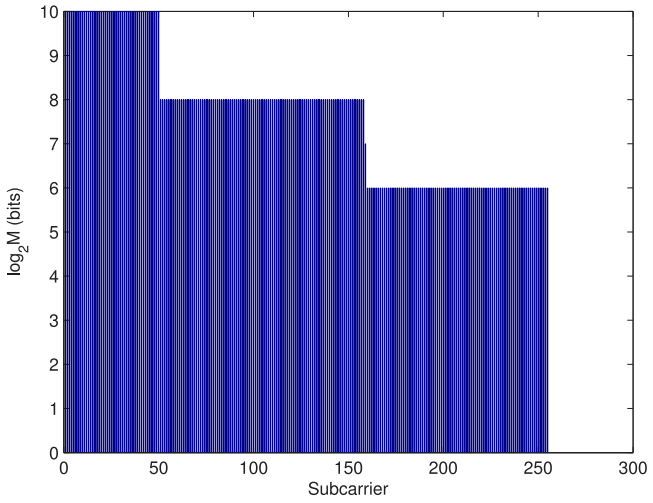

Fig. 6. Bits loaded on different subcarriers in the DCO-OFDM adaptive modulation system (SNR=75 dB, $\lambda = 2.5$, and receiver at $(1.5, 2.5, 1)$).

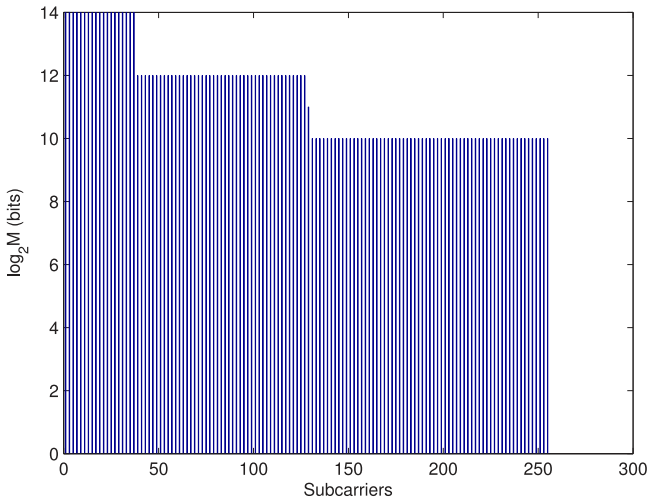

Fig. 7. Bits loaded on different subcarriers in the ACO-OFDM adaptive modulation system (SNR=75 dB and receiver at $(1.5, 2.5, 1)$).

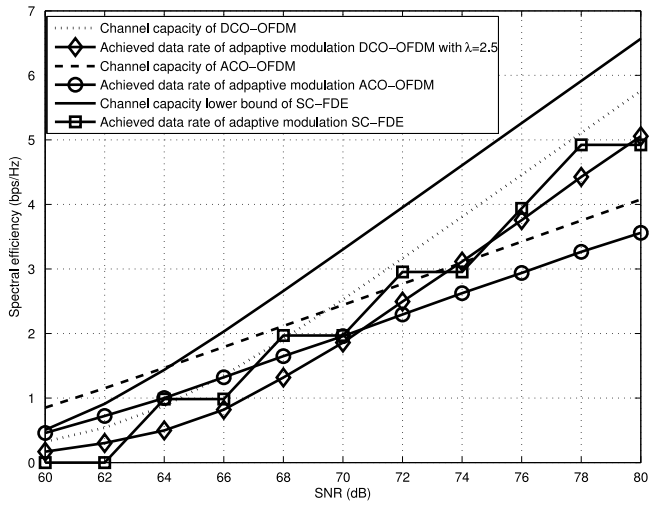

Fig. 8. Spectral efficiency of the three adaptive modulation schemes (receiver at $(1.5, 2.5, 1)$).

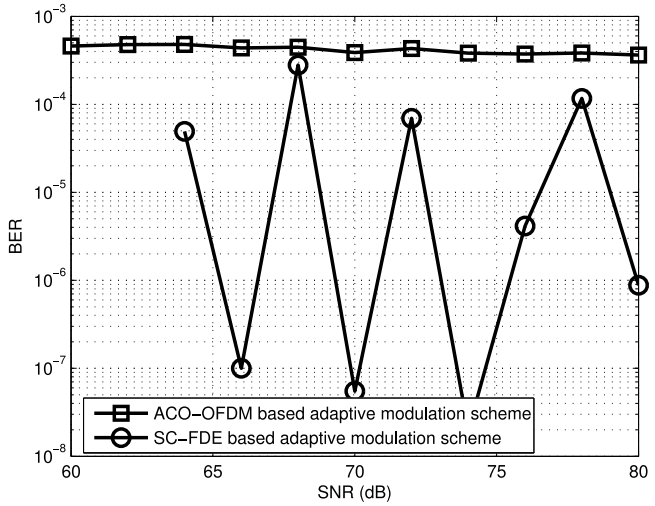

Fig. 9. BER of the ACO-OFDM and SC-FDE adaptive modulation systems. (receiver at $(1.5, 2.5, 1)$).

shows the loaded bits of different subcarriers in the ACO-OFDM system with adaptive modulation, and the same characteristics as the DCO-OFDM adaptive modulation system are observed. Simulation result shows that the number of bits carried by N consecutive PAM symbols in the SC-FDE adaptive modulation system is a constant, and 16-PAM is employed by the N consecutive PAM symbols when SNR=75 dB and the receiver is located at $(1.5, 2.5, 1)$.

Fig. 8 shows the channel capacity and the achieved spectral efficiency of ACO-OFDM VLC systems with adaptive modulation. The receiver is located at $(1.5, 2.5, 1)$. For comparison, the performance of the DCO-OFDM scheme with $\lambda = 2.5$ is also included. It is observed from that the channel capacity and the achieved spectral efficiency of the ACO-OFDM VLC system are higher than that of the DCO-OFDM VLC system in the low-SNR region. However, the DCO-OFDM VLC system is superior to the ACO-OFDM VLC system in the high SNR region.

The channel capacity lower bound of the SC-FDE VLC system and the achieved spectral efficiency of the PAM SC-FDE adaptive modulation VLC system are also plotted in Fig. 8. Results show that compared with the DCO-OFDM VLC system, the SC-FDE VLC system has a higher channel capacity. When adaptive modulation is employed, the performance of SC-FDE VLC system is better than that of the DCO-OFDM VLC system. Additionally, compared with OFDM based adaptive modulation schemes, the SC-FDE based adaptive modulation system requires much less feedback information and has a much lower complexity.

Fig. 9 shows the simulated BER performances of ACO-OFDM and SC-FDE adaptive modulation schemes assuming the same simulation environment adopted for Fig. 8. It shows that the BER target is met. Note that for the SC-FDE based

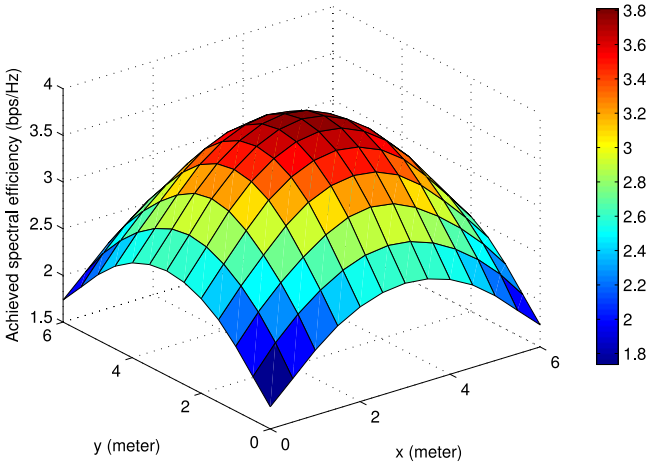

Fig. 10. Achieved spectral efficiency of the DCO-OFDM adaptive modulation system ($\lambda = 2.5$, SNR = 75 dB, and receiver is placed horizontally in the room at height of 1 meter above ground).

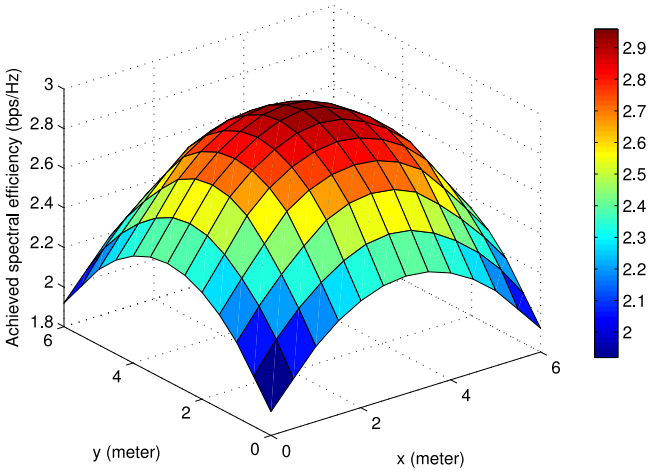

Fig. 11. Achieved spectral efficiency of the ACO-OFDM adaptive modulation system (SNR = 75 dB and receiver is placed horizontally in the room at height of 1 meter above ground).

scheme, the BER-SNR curves do not follow the usual trend as in a normal communications system without adaptive modulation. For example, the BER at SNR = 68 dB is higher than at SNR = 66 dB, because the achieved spectral efficiency at SNR = 68 dB is higher in the proposed adaptive modulation scheme as shown in Fig. 8. This means that the modulation order at SNR=68 dB is higher than at SNR = 66 dB.

Figs. 10–12 show the achieved spectral efficiency of the three adaptive modulation schemes, where the DC bias of the DCO-OFDM scheme is set at $2.5\sigma_x$ and the receiver is placed horizontally in the room at a height of 1 m above the ground with an SNR=75 dB. These results show that at such SNR value, the SC-FDE adaptive modulation scheme achieves the highest spectral efficiency, and the achieved spectral efficiency of the ACO-OFDM adaptive modulation scheme is the lowest. When the receiver is located at the center of the room, all three schemes reach their respective highest spectral efficiency.

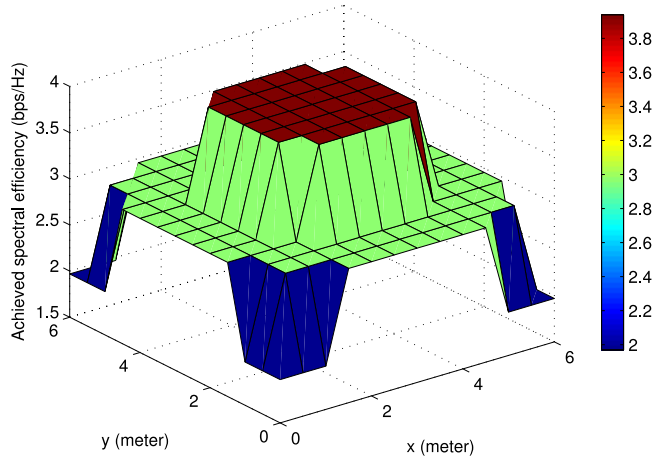

Fig. 12. Achieved spectral efficiency of the SC-FDE adaptive modulation system (SNR = 75 dB and receiver is placed horizontally in the room at height of 1 meter above ground).

Note that all the analyses have assumed a perfect feedback channel. While an in-depth analysis of the effects of a practical quantized feedback channel is beyond the scope of this work, quantized CSI will affect the system performance. The achieved spectral efficiency of the proposed adaptive modulation schemes presented in this paper can be viewed as the upper bound of the system using a quantized feedback channel. The feedback information for the SC-FDE based adaptive modulation scheme is communicated in a quantized way naturally since only the modulation order needs to be sent back. Depending on the application, both RF and VLC can be used as the medium for feedback.

V. Conclusion

We have proposed three adaptive modulation schemes for high speed VLC systems. The OFDM based adaptive modulation schemes use optimal bit loading to adjust the modulation order and power allocation according to the channel conditions. In the low-SNR region, the performance of the ACO-OFDM based adaptive modulation scheme is better than that of the DCO-OFDM based adaptive modulation scheme. The information rate of the OFDM based schemes assuming a constant transmit power is also analyzed. The SC-FDE based adaptive modulation scheme achieves a better performance than the DCO-OFDM based scheme. The required feedback information for the SC-FDE based scheme is much less than that for the OFDM based schemes. Furthermore, the demodulation complexity of the SC-FDE scheme is lower than that of the OFDM based schemes, because SC-FDE employs the same modulation scheme in one frame, whereas the OFDM based schemes use different modulation schemes for different subcarriers.

References

[1] T. Komine and M. Nakagawa, "Fundamental analysis for visible-light communication system using LED lights," *IEEE Trans. Consumer Electron.*, vol. 50, no. 1, pp. 100–107, Feb. 2004.

[2] H. Elgala, R. Mesleh, and H. Haas, "Indoor optical wireless communication: Potential and state-of-art," *IEEE Commun. Mag.*, vol. 49, no. 9, pp. 56–62, Sep. 2011.
[3] L. Zeng, D. O'Brien, H. Le-Minh, K. Lee, D. Jung, and Y. Oh, "Improvement of date rate by using equalization in an indoor visible light communication system," in *Proc. IEEE Int. Conf. Circuits Syst. Commun.*, May 2008, pp. 678–682.
[4] M. Biagi, T. Borogovac, and T. D. C. Little, "Adaptive receiver for indoor visible light communicationsx," *J. Lightw. Technol.*, vol. 31, no. 23, pp. 3676–3686, Dec. 2013.
[5] J. B. Carruthers and J. M. Kahn, "Multiple-subcarrier modulation for nondirected wireless infrared communication," *IEEE J. Sel. Areas Commun.*, vol. 14, no. 3, pp. 538–546, Apr. 1996.
[6] J. Armstrong and A. Lowery, "Power efficient optical OFDM," *Electron. Lett.*, vol. 42, no. 6, pp. 370–372, Mar. 2006.
[7] N. Zervos and I. Kalet, "Optimized decision feedback equalization versus optimized orthogonal frequency division multiplexing for high-speed data transmission over the local cable network," in *Proc. IEEE Int. Conf. Commun.*, 1989, pp. 1080–1085.
[8] P. S. Chow, J. M. Cioffi, and J. A. C. Bingham, "A practical discrete multitone transceiver loading algoritm for data transmission over spectrally shaped channels," *IEEE Trans. Commun.*, vol. 43, no. 2–4, pp. 772–775, Feb.–Apr. 1995.
[9] A. Czylwik, "Adaptive OFDM for wideband radio channels," in *Proc. IEEE Global Telecommun. Conf.*, Nov. 1996, pp. 713–718.
[10] Z. Zhou, B. Vucetic, M. Dohler, and Y. Li, "MIMO systems with adaptive modulation," *IEEE Trans. Veh. Technol.*, vol. 54, no. 5, pp. 1828–1842, Sep. 2005.
[11] O. Gonzalez, R. Perez-Jimenez, S. Rodriguez, J. Rabadan, and A. Ayala, "Adaptive OFDM system for communications over the indoor wireless optical channel," *IEE Proc.-Optoelectron.*, vol. 153, no. 4, pp. 139–144, Aug. 2006.
[12] V. Jungnickel, V. Pohl, S. Nonnig, and C. V. Helmolt, "A physical model of the wireless infrared communication channel," *IEEE J. Sel. Areas Commun.*, vol. 20, no. 3, pp. 631–640, Aug. 2002.
[13] J. M. Kahn and J. R. Barry, "Wireless infrared communications," *Proc. IEEE*, vol. 85, no. 2, pp. 265–298, Feb. 1997.
[14] J. R. Barry, *Wireless Infrared Communications*. Norwell, MA, USA: Kluwer, 1994.
[15] J. Armstrong and B. J. C. Schmidt, "Comparison of asymmetrically clipped optical OFDM and DC-biased optical OFDM in AWGN," *IEEE Commun. Lett.*, vol. 12, no. 5, pp. 343–345, May 2008.
[16] L. Chen, B. Krongold, and J. Evans, "Performance analysis for optical OFDM transmission in short-range IM/DD systems," *J. Lightw. Technol.*, vol. 30, no. 7, pp. 974–983, Apr. 2012.
[17] S. Dimitrov, S. Sinanovic, and H. Haas, "Clipping noise in OFDM-based optical wireless communication systems," *IEEE Trans. Commun.*, vol. 60, no. 4, pp. 1072–1081, Apr. 2012.
[18] S. Dimitrov and H. Haas, "Information rate of OFDM-based optical wireless communication systems with nonlinear distortion," *J. Lightw. Technol.*, vol. 31, no. 6, pp. 918–929, Mar. 2013.
[19] D. Tse and P. Viswanath, *Fundamentals of Wireless Communication*. Cambridge, U.K.: Cambridge Univ. Press, 2005.
[20] X. Li, R. Mardling, and J. Armstrong, "Channel capacity of IM/DD optical communication systems and of ACO-OFDM," in *Proc. IEEE Int. Conf. Commun.*, Jun. 2007, pp. 2128–2133.
[21] S. Zhou and G. Giannakis, "Adaptive modulation for multi-antenna transmissions with channel mean feedback," *IEEE Trans. Wireless Commun.*, vol. 3, no. 5, pp. 1626–1636, Sep. 2004.
[22] J. Campello, "Optimal discrete bit loading for multicarrier modulation systems," in *Proc. IEEE Int. Symp. Inform. Theory*, Aug. 1998, p. 193.
[23] M. Wolf, L. Grobe, M. R. Rieche, A. Koher, and J. Vucic, "Block transmission with linear frequency domain equalization for dispersive optical channels with direct detection," in *Proc. Int. Conf. Transparent Opt. Netw.*, Jun. 2010, pp. 1–8.
[24] A. Lapidoth, S. M. Moser, and M. A. Wigger, "On the capacity of free-space optical intensity channels," *IEEE Trans. Inform. Theory*, vol. 55, no. 10, pp. 4449–4461, Oct. 2009.

Liang Wu (M'13) received the B.S., M.S., and Ph.D. degrees, all from the School of Information Science and Engineering, Southeast University, Nanjing, China. From September 2011 to March 2013, he was with the School of Electrical Engineering and Computer Science, Oregon State University, as a Visiting Student. He is currently a Lecturer with the National Mobile Communications Research Laboratory, Southeast University. His research interests include ultra-wideband wireless communication system, indoor optical wireless communications, massive multiple-input and multiple-output wireless communication systems, and interference cancellation techniques.

Zaichen Zhang (M'02) received the B.S. and M.S. degrees in electrical and information engineering from Southeast University, Nanjing, China, in 1996 and 1999, respectively, and the Ph.D. degree in electrical and electronic engineering from the University of Hong Kong, Hong Kong, in 2002. From 2002 to 2004, he was a Postdoctoral Fellow at the National Mobile Communications Research Laboratory, Southeast University. He is currently a Professor at Southeast University. He is also a Visiting Professor at Nantong University, Nantong, China. His current research interests include ultra-wideband technology, visible light communications, and new generation wireless communication systems.

Jian Dang received the B.S. and Ph.D. degrees from the School of Information Science and Engineering, Southeast University, Nanjing, China. He is currently a Lecturer with the National Mobile Communications Research Laboratory, Southeast University. From September 2010 to March 2012, he was with the Department of Electrical and Computer Engineering, University of Florida, as a Visiting Student. His research interests include signal processing in wireless communications, multiple access schemes, nonorthogonal modulation schemes and visible light communications.

Huaping Liu (SM'08) received the B.S. and M.S. degrees in electrical engineering from the Nanjing University of Posts and Telecommunications, Nanjing, China, in 1987 and 1990, respectively, and the Ph.D. degree in electrical engineering from the New Jersey Institute of Technology, Newark, NJ, USA, in 1997. From July 1997 to August 2001, he was with Lucent Technologies, Whippany, NJ, USA. Since September 2001, he has been with the School of Electrical Engineering and Computer Science, Oregon State University, Corvallis, OR, USA, where he is currently a Professor. His research interests include ultra-wideband systems, multiple-input multiple-output antenna systems, channel coding, and modulation and detection techniques for multiuser communications.